Extended coupled channel method for baryon scattering based on the dynamics of the Bohr Hamiltonian deduced from a microscopic nucleon-nucleon Hamiltonian

Krishna Kumar
Physics Department, Tennessee Technological University, Cookeville, Tennessee 38505

Ch. Lagrange and M. Girod
Service de Physique Neutronique et Nucleaire, 91680 Bruyeres-Le-Chatel, France

B. Grammaticos
Centre de Recherches Nucléaires de Strasbourg, 67037 Strasbourg, France
(Received 29 October 1984)

The coupled channel method has been extended so as to include the possibilities of spherical-transitional-deformed target nuclei, different shapes for target and final nuclei, and different shapes for different reaction channels. Deformation-dependent nuclear structure wave functions, solutions of a Bohr Hamiltonian deduced from a microscopic Hamiltonian, are employed to weigh the scattering potentials for different shapes and channels. The deformation and K-dependent form factors are integrated over deformation variables and summed over K in a general theory applicable to a wide variety of targets and projectiles. Illustrative examples, including comparisons with experimental cross sections, are presented for ^{4}He scattering from ^{24}Mg and ^{28}Si, and for total neutron cross sections of ^{148,150,152,154}Sm.

I. INTRODUCTION

In recent years, much effort has been devoted to combining the nuclear structure methods for the bound states with the nuclear reaction methods for the scattering form factors.[1] It is generally well recognized that although the optical potential provides a reasonable alternative to the cumbersome and time-consuming calculation of the overlaps of the microscopically calculated single-particle wave functions, it by itself is not adequate for a satisfactory description of the rich variety of data available for baryon (n, p, ^{4}He, . . .) scattering. In his pioneering paper, Tamura[2] proposed and applied the coupled channel method (CCM) which combines the optical model for nuclear reactions with the Bohr-Mottelson model[3] for nuclear structure. This approach was further extended by Rebel *et al.*[4] who replaced the Bohr-Mottelson model by the Frankfurt model.[5] This was a great improvement over the earlier CCM since the target nucleus could be close to one of the limits (vibrational or rotational) of the Bohr-Mottelson model or it could be anywhere in between (transitional or soft against shape fluctuations, or a nucleus with the coexistence of very different shapes at different excitations). However, the parameters of the collective Hamiltonian had to be determined for each nucleus by fitting the low-energy collective states which may not represent all the necessary details of the underlying microscopic structure.

In the present approach, we attempt to go one step closer to the first principles by employing the dynamics of the Bohr Hamiltonian[6] deduced from a microscopic nucleon-nucleon Hamiltonian. Since the microscopic information does not enter directly in our calculation of the baryon scattering form factors, our method would appear on the surface to be the same as that employed by Rebel *et al.* The numerical results might very well turn out to be quite similar in some cases. But there are several important differences from a conceptual as well as a practical point of view: (1) One of these is that while Rebel *et al.* employ an expansion around the spherical shape, we avoid such an expansion completely.[7] In fact, the latest version of our nuclear structure program has been extended to deformations approaching infinity and leading to fission.[8] (2) Secondly, while the Frankfurt model employed by Rebel *et al.* requires a large number of fitting parameters per nucleus, all parameters of our structure calculation have previously prescribed strengths and Z-A dependences.

The two main approximations of our calculation of baryon scattering rate are the following: (1) The adiabatic approximation is utilized to write the total nuclear wave function as a product of an intrinsic wave function and a collective wave function. (2) The expectation value of the scattering operator with respect to the intrinsic wave function (corresponding to a certain shape) is approximated by the optical potential. These approximations are discussed in more detail in Sec. II, where the salient points of the CCM are also reviewed.

The main points of two versions of our nuclear structure program are discussed in Sec. III. One of these is based on the Hartree-Fock-Bogoliubov (HFB) treatment of a density-dependent nucleon-nucleon interaction in a large configuration space.[9,10] The other version is based on the dynamic deformation model (DDM) where the Nilsson-Strutinsky method is combined with the Bogoliubov treatment of the residual (pairing) nucleon-nucleon interaction.[7] In both cases the collective wave functions, employed in the calculation of the form factors, are com-

puted by employing the Kumar-Baranger method of solving the Bohr Hamiltonian.[11,12]

The choice of the method of calculation of the collective wave functions dictates the manner in which the optical potential depending on the nuclear surface is treated. In Sec. IV, we discuss our method of including the nuclear shape (β, γ) dependence of the optical potential, the corresponding determination of the multipole components via a two-dimensional integration over the angles (θ,φ), and the extension of the CCM for baryon scattering form factors.

A few numerical examples indicating the versatility of our approach, as well as agreement with the experimental cross sections, are discussed in Sec. V. Our conclusions are presented in Sec. VI.

Some of the numerical results discussed in the following have previously been presented at a number of conferences.[13–15]

II. BASIC IDEAS AND APPROXIMATIONS OF THE EXTENDED COUPLED CHANNEL METHOD

A. Brief review of the coupled channel formalism

In order to clarify the notations used in the following, we start by reminding the reader of the salient points of the coupled channel formalism.[2]

The projectile-target Hamiltonian is written as

$$H=T+H_t+V(r,\theta,\varphi)\ , \tag{1}$$

where T is the projectile kinetic energy, H_t is the Hamiltonian for the internal motion of the target, V is the projectile-target interaction, and (r,θ,φ) are the projectile coordinates relative to the center of mass of the target. The corresponding Schrödinger equation is written as

$$H\Psi=E_1\Psi\ , \tag{2}$$

where E_1 is the projectile energy in the center-of-mass system. The total wave function Ψ is written in the angular-momentum-coupled representation as (in order to simplify the notation, we have dropped the subscript n, as compared to Tamura, as much as possible)

$$\Psi=r^{-1}\sum_{Jnlj}R_{Jnlj}(r)[\,|\,lj\rangle\otimes|\,nI\rangle]_{JM}\ , \tag{3}$$

where J is the total angular momentum of the projectile-target system, M is the projection of $\mathbf{J}$ on the laboratory z axis, $|\,nI\rangle$ represents the nth target state with angular momentum $\mathbf{I}$, and $|\,lj\rangle$ is the $(l,s)j$-coupled generalized spherical harmonic for the projectile. The target wave function $|\,nIM_t\rangle$ represents a solution of the target Schrödinger equation,

$$H_t\,|\,nIM_t\rangle=W_n\,|\,nIM_t\rangle\ , \tag{4}$$

where W_n is the target energy. Note that the index n is a collective index for all relevant target quantum numbers (I, parity, . . .) except for the magnetic one.

Following Tamura,[2] we divide the interaction V into a diagonal part, $V_{\rm diag}$, which represents the interaction of the projectile with the target in its spherical shape, and a nondiagonal part $V_{\rm coupl}$, which represents the interaction caused by the deformation of the target. The angular parts of the diagonal part of the Schrödinger equation (2), are integrated out in the usual way, and then one gets the basic equation of the coupled channel formalism,[2]

$$\{(d^2/d\rho_n^2)-[l(l+1)/\rho_n^2]-(V_{\rm diag}/E_n)+l\}R_{Jnlj}(r)$$
$$=(l/E_n)\sum_{n'l'j'}\langle(\,|\,lj\rangle\otimes|\,nI\rangle)_{JM}$$
$$|\,V_{\rm coupl}\,|(\,|\,l'j'\rangle\otimes|\,n'I'\rangle)_{JM}\rangle R_{Jn'l'j'}(r)\ , \tag{5}$$

where $\rho_n=k_nr$, k_n is the wave number, and E_n $(=E_1-W_n)$ is the energy of the ejectile which leaves the target in its nth state.

Equation (5) of the coupled channel method represents a set of coupled equations and is quite general. It holds irrespective of the nature of the projectile or of the target nucleus. Assumptions about the nuclear structure affect only the matrix elements which appear on the right-hand side of the equation, and the evaluation of those matrix elements is the most crucial part of the whole calculation.

This evaluation requires two main approximations. One of them refers to the target nucleus wave functions, the solutions of Eq. (4). The other one refers to the coupling potential, $V_{\rm coupl}$. These approximations are discussed in the following.

B. Main approximations of the method

1. *The adiabatic approximation*

The target wave function of Eq. (4) can be written as,

$$|\,nIM_t\rangle=\sum_K\Phi^I_{M_t,k}\,|\,nIK\rangle\ , \tag{6}$$

where K is the projection of $\mathbf{I}$ on the intrinsic (body-fixed) z axis and Φ is the symmetrized rotational function[11] depending on the three Euler angles between the laboratory and the intrinsic axes. Equation (6) represents the transformation from one set of axes to another and is exact as long as the summation over K is performed over all the $(2I+1)$ values.

The adiabatic approximation is now invoked to write

$$|\,nIK\rangle=\sum_i A_{nIK}(\beta_i,\gamma_i)\chi(\beta_i,\gamma_i,x_j)\ , \tag{7}$$

where i is an index for different values of the shape variables (β_i,γ_i), A_{nIK} represents a purely collective wave function depending on the shape variables only, and χ represents the intrinsic-microscopic wave function depending on the nucleon variables x_j $(j=1,3A)$ as well as on the shape variables. Note that the shape variables (β_i,γ_i) may be related to the expectation values of the quadrupole operators $\langle Q_{20}\rangle$, $\langle Q_{22}+Q_{2,-2}\rangle$, or equivalently to $\langle x^2\rangle$, $\langle y^2\rangle$, $\langle z^2\rangle$. The adiabatic approximation is involved in the assumption that the microscopic wave function does not depend explicitly on I or on K.

The approximation discussed previously is reminiscent of the adiabatic approximation inherent in the rotational model of Bohr and Mottelson.[3] However, our adiabatic approximation is much less restrictive because of the following. (1) The assumption of axial symmetry is dropped

and the K mixing is fully taken into account. This part of our approach is similar to that attained in the Davydov-Filippov model.[16] (2) The assumption of a fixed nuclear shape (employed in both the Bohr-Mottelson and in the Davydov-Filippov models) is dropped. The shape fluctuations and the corresponding rotation-vibration couplings are fully taken into account.

Another aspect of the adiabatic approximation concerns the treatment of the "extra" degrees of freedom. The product wave function of Eqs. (6) and (7) has five extra degrees of freedom (β,γ, three Euler angles). If we were to employ such a wave function to calculate only the potential energy $V(\beta,\gamma)$ as is done in many calculations based on the modified oscillator method (see, for example, Ref. 17) or on the Hartree-Fock method (see, for example, Ref. 18), then our calculation would definitely suffer from this problem. However, we correct for this problem by calculating not only $V(\beta,\gamma)$ but also six inertial functions (to be discussed in the following). The latter represent off-diagonal or nonlocal[19] terms in the language of the generator-coordinate method, while they represent time-dependent corrections due to shape fluctuations in the language of the cranking method.[20,21]

In our adiabatic approximation, the amplitudes of collective vibrations can be as large as necessary, but their time dependences (collective frequencies) are assumed to be small. This is just the opposite of the random phase approximation[22] where the amplitudes are assumed to be small but the frequencies can be large.

2. *The optical potential approximation*

The main ingredients needed for a fully microscopic calculation of the form factors are a complex effective target-projectile interaction together with the ground-state and transition nucleon density distributions. As the target nuclei considered here could be anywhere between the two limits (vibrational, rotational) of the Bohr-Mottelson model, a microscopic description of elastic and inelastic scattering cross sections using the adiabatic rotational model, valid only for the ground state bands of well-deformed nuclei (see, for examples of such calculations, Refs. 23 and 24) cannot be applied here. We have not undertaken a new microscopic calculation of scattering cross sections for the following reasons: (i) Problems occur for the validity (or choice) of a folding procedure in the case of alpha-nucleus interaction. (ii) Calculations of nucleon density distributions for all the allowed transitions between the various collective bands are rather impractical. We mention that a fully microscopic calculation of proton scattering from the ground state rotational bands of s-d shell nuclei was presented by the Oxford group.[25,26] Furthermore, a more general and fully microscopic treatment of the projectile-target interaction has been formulated.[27] It has been applied in a truncated configuration space of two oscillator shells to the problem of two-nucleon-transfer cross sections.[28] That microscopic calculation of the overlaps of various single-particle wave functions for different shapes was already quite large. It would be much too large for the largest computers that are currently available due to the greatly expanded configuration space of present calculations.

III. THE BOHR HAMILTONIAN AND ITS DEDUCTION FROM MICROSCOPIC THEORIES

A. The Bohr Hamiltonian

The original Bohr Hamiltonian for the quadrupole motion was given for the case of small amplitude, harmonic vibrations around the spherical shape.[6] A more general form, valid for spherical-transitional-deformed nuclei, is[11]

$$H_t = V(\beta,\gamma)+(\tfrac{1}{2})\left[B_{00}(\beta,\gamma)\dot{\beta}_0^2+2B_{02}(\beta,\gamma)\dot{\beta}_0\dot{\beta}_2 +B_{22}(\beta,\gamma)\dot{\beta}_2^2+\sum_k I_k^2/\mathcal{I}_k(\beta,\gamma)\right], \tag{8}$$

where (β,γ) are the quadrupole shape variables,[6]

$$\beta_0=\beta\cos\gamma,\quad \beta_2=\beta\sin\gamma\ , \tag{9}$$

k ($=1,2,3$ or $=x,y,z$) represents the three intrinsic (body-fixed) axes, V is the potential energy of nuclear deformation, B_{mn} (m or $n=0,2$) are the vibrational mass parameters, and $\mathcal{I}_k$ are the rotational moments of inertia.

The Bohr Hamiltonian of Eq. (8) is determined completely by seven functions of β and γ, namely the potential function V and the six inertial functions: B_{00}, B_{02}, B_{22}, $\mathcal{I}_1$, $\mathcal{I}_2$, and $\mathcal{I}_3$. These functions must obey certain stringent symmetry conditions in order to satisfy invariance under rotations, and invariance under different ways of labeling or orienting the intrinsic axes with respect to the laboratory axes.[6,11] Although a microscopic calculation of the seven functions in a large configuration space requires a considerable amount of computational effort, such a calculation has two incomparable advantages over nonmicroscopic calculations: (1) All the symmetry conditions mentioned already are satisfied automatically. (2) Expansions around either the spherical shape or around a deformed shape are avoided completely.

The Bohr Hamiltonian of Eq. (8) is solved numerically on the basis of Eqs. (6) and (7). Deviations from axial symmetry and from the ground state shapes are fully taken into account. The so-called shape coexistence and band mixing arise naturally in this model of collective quadrupole motion.[7,11,12]

Two different microscopic methods of calculating the seven functions have been developed because of the following reasons: The more fundamental (HFB) method requires more computation time by a factor of 5—20. Hence, it is not practical to use this method for a global study of light-medium-heavy nuclei such as that presented for the structure properties.[7,13] Moreover, the microscopic method based on the dynamic deformation model (DDM) includes pair fluctuations, which are not included in the HFB method. Attempts are in progress to replace the model by a theory, which will probably be closer to the HFB theory. The main ideas behind the two methods are summarized in the following.

B. The Hartree-Fock-Bogoliubov calculation of the seven functions of deformation

As mentioned in the Introduction, the first method we have used for the description of the structure of the nucleus is the Hartree-Fock-Bogoliubov method. In this method the nuclear wave function is given by a HFB (independent quasiparticle) form. The finite-range effective interaction ($D1$) of Dechargé and Gogny[9] is used in order to describe the interaction between nucleons in the mean field approximation. Two important features of our calculation must be pointed out here. First, the description of the pairing part of the nuclear interaction is obtained in a fully self-consistent manner. This is achieved through the use of the HFB theory together with an interaction, like $D1$, which has the desirable pairing properties. Second, all the nucleons are treated on an equal footing: no assumption whatsoever is made about the existence of an inert core.

In the HFB theory we have used, we start with the most general Bogoliubov transformation in the nucleon creation and annihilation operators $a^{\dagger}_{\alpha}, a_{\alpha}$,

$$\xi^{\dagger}_{\lambda} = \sum_{\alpha} (u^{\lambda}_{\alpha} a^{+}_{\alpha} + v^{\lambda}_{\alpha} a_{\alpha}) . \tag{10}$$

Introducing the density matrix and the pairing tensor,

$$\rho_{\delta\beta} = \sum_{\lambda} v^{\lambda}_{\beta} v^{\lambda}_{\delta} , \tag{11}$$

$$\chi_{\bar{\delta}\beta} = \sum_{\lambda} u^{\lambda}_{\bar{\delta}} v^{\lambda}_{\beta} , \tag{12}$$

(where $\bar{\delta}$ denotes the time reversed of the state δ), we can write the total nuclear energy as

$$\begin{aligned} \langle \tilde{0} | H | \tilde{0} \rangle = & \sum_{\alpha\gamma} \langle \alpha | t | \gamma \rangle \rho_{\alpha\gamma} \\ & + (\tfrac{1}{2}) \sum_{\alpha\beta\gamma\delta} \langle \alpha\beta | V | \gamma\tilde{\delta} \rangle \rho_{\beta\delta} \rho_{\alpha\gamma} \\ & + (\tfrac{1}{4}) \sum_{\alpha\beta\gamma\delta} \langle \alpha\bar{\gamma} | V | \beta\tilde{\bar{\delta}} \rangle \kappa_{\bar{\delta}\beta} \kappa_{\alpha\bar{\gamma}} , \end{aligned} \tag{13}$$

where H is the nuclear Hamiltonian and $|\tilde{0}\rangle$ is the HFB wave function. The application of the variational principle on the energy $\langle \tilde{0} | H | \tilde{0} \rangle$ with the constraint $-\lambda N$, for the mean particle number to be conserved, leads to the HFB equations. Their matrix form is

$$\begin{bmatrix} \epsilon_{\alpha\gamma} & \Delta_{\alpha\bar{\gamma}} \\ -\Delta_{\bar{\alpha}\gamma} & -\epsilon_{\bar{\alpha}\bar{\gamma}} \end{bmatrix} \begin{bmatrix} u_{\gamma} \\ v_{\gamma} \end{bmatrix} = e_{\alpha} \begin{bmatrix} u_{\alpha} \\ \bar{v}_{\alpha} \end{bmatrix} , \tag{14}$$

where $\epsilon_{\alpha\gamma} = t_{\alpha\gamma} - \lambda\delta_{\alpha\gamma} + \Gamma_{\alpha\gamma}$, Γ and Δ being the Hartree-Fock field and the pairing field, respectively.

In the constrained-triaxial-HFB calculations that we have performed, the constraints on the two quadrupole moments, Q_{20}, Q_{22} are included in ϵ. In that way, the shape of the nucleus can be chosen freely in the β,γ plane. The expansion associated with the index α in Eq. (10) is over a Cartesian oscillator basis which incorporates the triaxial symmetry. (For all technical details, see Ref. 29.) The energy of the nucleus can be computed via Eq. (13) as a function of the deformation variables β and γ. However, in order to use this energy as a collective potential in a dynamical calculation, zero-point energy corrections must be included. They can be deduced in the framework of the generator coordinate theory and have been presented in detail in Ref. 30. The same method (which is considerably improved compared to our previous calculation[10] for ^{150}Sm) has been employed in the HFB calculations presented in the following.

The collective potentials thus obtained for ^{24}Mg, ^{28}Si, ^{150}Sm, and ^{152}Sm are displayed in Figs. 1–4. All these nuclei possess an equilibrium shape which is axially deformed (prolate for Mg and Sm, oblate for Si). However, all the nuclei present a softness in the γ direction which makes mandatory the use of a dynamical description of the nucleus.

The other ingredients of the present dynamical theory are the inertial parameters associated with the quadrupole vibrations and the rotations. In the adiabatic approximation, the inertial parameters are given by the "cranking" theory. The vibrational mass parameters B_{00}, B_{02}, and B_{22} are obtained by using HFB wave functions and taking into account the coupling between Q_{20} and Q_{22} vibrations.

The moments of inertia are given by the familiar cranking expression

$$\mathcal{I}_k = 2\hbar^2 \sum_{\alpha\beta} | \langle \alpha\beta | J_k | \phi_q \rangle |^2 / (e_{\alpha} + e_{\beta}) , \tag{15}$$

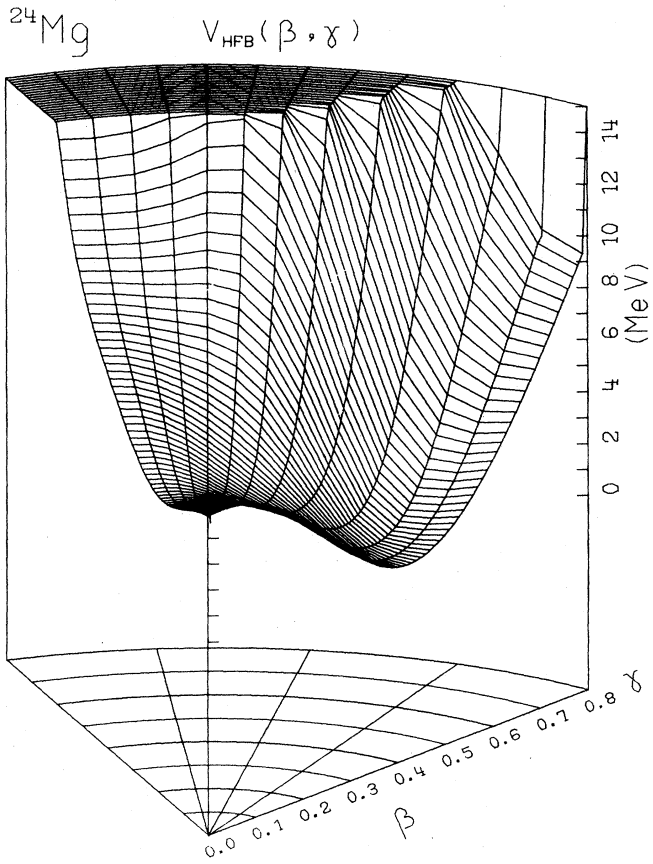

FIG. 1. HFB potential $V(\beta,\gamma)$ of ^{24}Mg. The shape asymmetry variable γ varies from 0° on the right to 60° on the left of the curved axes perpendicular to the β axis.

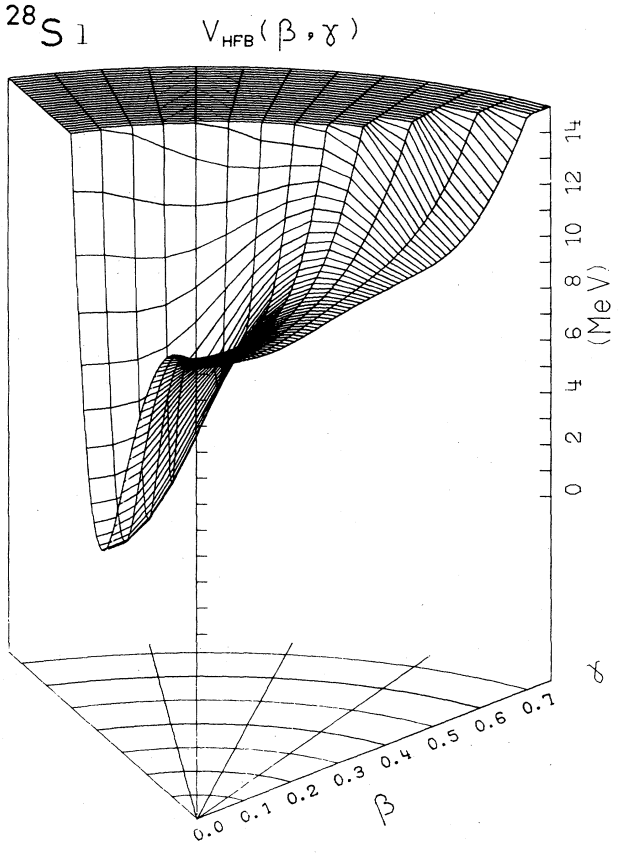

FIG. 2. HFB potential $V(\beta,\gamma)$ of ^{28}Si. See Fig. 1 caption for the explanation of the γ axis.

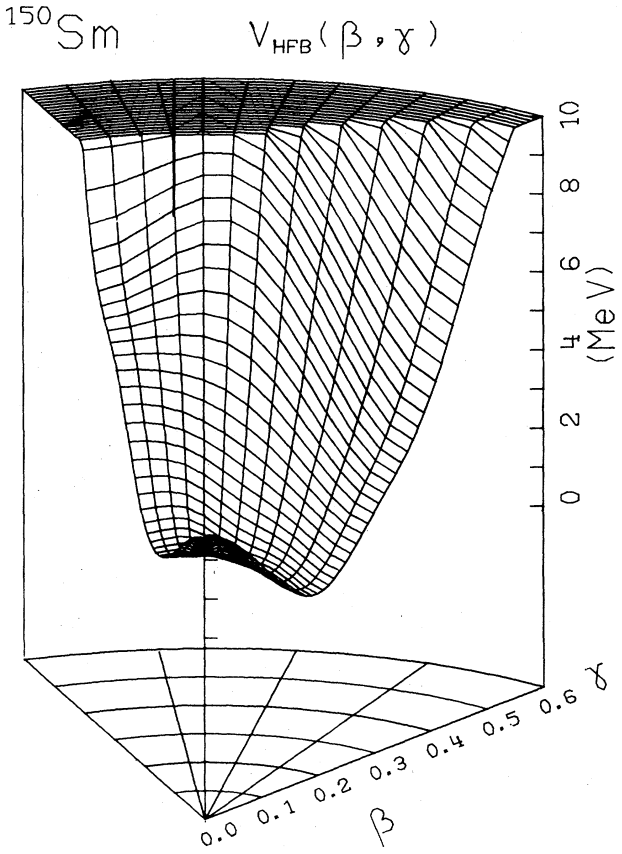

FIG. 3. HFB potential $V(\beta,\gamma)$ of ^{150}Sm. See Fig. 1 caption for the explanation of the γ axis.

where $|\phi_q\rangle$ is the intrinsic state.

In the case of the ^{152}Sm nucleus, the inertial parameters B_{00}, B_{02}, and B_{22} are displayed in Figs. 5—7 as functions of β and γ. We remark that the inertial parameters present substantial variations and are far from being constant.

It is worthwhile to state that the calculation of the collective functions is fully microscopic and does not contain any adjustable parameters. Once the nuclear interaction is chosen (in this case the Gogny $D1$ interaction), the HFB calculation furnishes the collective potential and masses in a systematic way and, hence, the collective spectrum.

C. The dynamic deformation model calculation of the seven functions of deformation

The second microscopic method employed for the calculation of the seven functions of the Bohr Hamiltonian also requires the solution and use of Eqs. (10)—(15) given previously. However, the computation is simplified greatly because the lengthy iterative-HFB calculation for each nucleus is replaced by a single calculation (for the deformed single-particle states) for all nuclei, followed by a comparatively small calculation for each nucleus.

The main simplifying assumptions are the following: (1) The low-energy spectra of odd nuclei near doubly-magic nuclei provide the needed spherical single-particle energies. (2) The corresponding wave functions are simply the harmonic oscillator wave functions including spin-orbit coupling. (3) Effects of deformation can be taken into account by allowing the oscillator frequencies to be different in different directions. (4) The residual nucleon-nucleon interaction can be approximated by the Bardeen-Cooper-Schrieffer (BCS) pairing force.

With these assumptions, the generalized Bogoliubov transformation of Eq. (10) splits into two parts—one from spherical to deformed single-particle states, the other one from single-particle to quasiparticle states. It is still necessary to diagonalize the deformation effects in the full configuration space (divided roughly by a factor of 4 because of conservation of parity and of time-reversal invariance), but the doubling of the space required by the full HFB Eq. (14) is avoided.

One additional assumption is made in the calculation of the nuclear energy of Eq. (13). The exchange term is neglected. Instead, a modified Strutinsky shell-correction method[31] is employed and the potential energy function is written as[7]

$$V = V_{\rm DM} + \delta U + V_P + V_{\rm proj} , \tag{16}$$

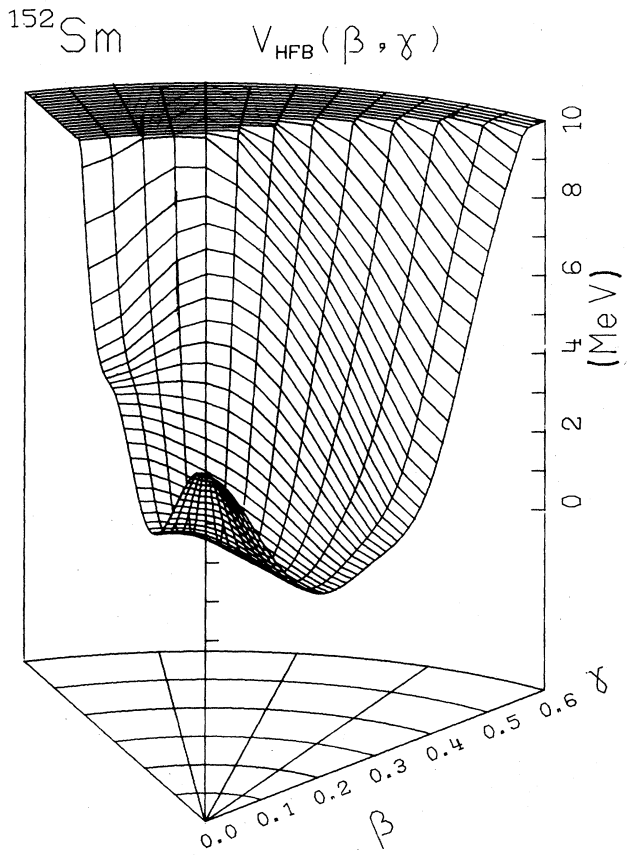

FIG. 4. HFB potential $V(\beta,\gamma)$ of ^{152}Sm. See Fig. 1 caption for the explanation of the γ axis.

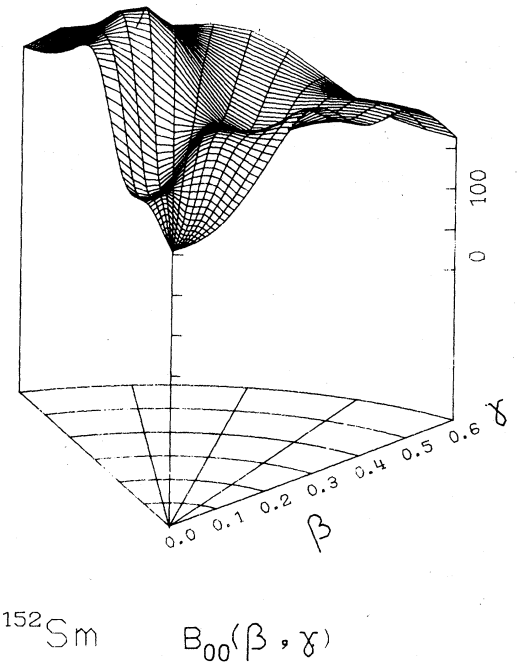

FIG. 5. Inertial function $B_{00}(\beta,\gamma)$ of ^{152}Sm. The function values are in units of $\hbar^2$(MeV)$^{-1}$. See Fig. 1 caption for the explanation of the γ axis.

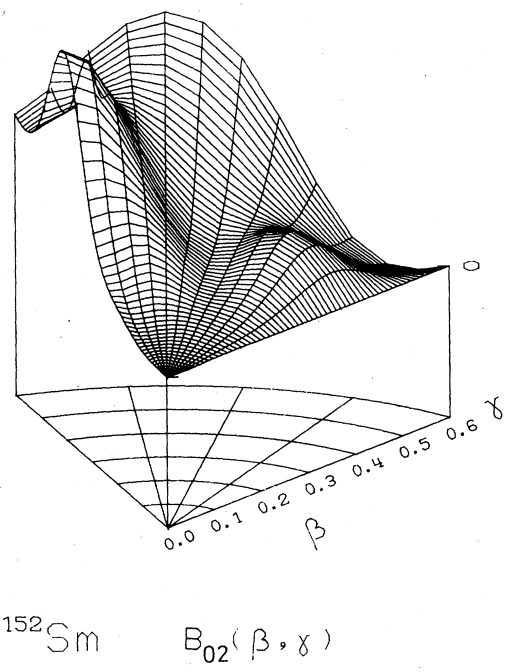

FIG. 6. Inertial function $B_{02}(\beta,\gamma)$ of ^{152}Sm. See Fig. 5 caption for further details.

where $V_{\rm DM}$ is the droplet model[32] energy, δU is the shell correction, V_P is the pairing correction, and $V_{\rm proj}$ is the nine-dimensional (three for rotations, two for β-γ vibrations, two for pair fluctuations, and two for particle-number fluctuations) projection correction.

The pair- and particle-number fluctuations affect not only the potential energy of deformation, but also the six inertial functions of the Bohr Hamiltonian of Eq. (8). These effects have been deduced via a nine-dimensional generalization of the original cranking constraint,[20] $-\omega J_x$, where ω is the rotational frequency for rotation around the intrinsic x axis. The nine constraints are treated via second-order time-dependent perturbation theory. This method has two great advantages over the direct inclusion of such a constraint term in the single-particle basis: (1) The nine-dimensional equivalents of the constraint condition $\langle J_x \rangle = \omega \mathcal{I}$ are automatically satisfied up to the order considered. Thus, many numerical problems of the "exact" (direct-inclusion) method are avoided completely. (2) Although a perturbation expansion in the collective frequencies (or velocities) is made, this expansion is made not just around the potential minimum but around each point of a two-dimensional (β-γ) mesh. This is similar to modern methods of numerical integrations which employ perturbation expansions around mesh points, but yield exact results (to some prescribed numerical accuracy). Nevertheless, the present method is not valid at very high spins where the rotational frequency becomes comparable to one or more of the frequencies of the single-particle field.

The calculation of the seven functions is performed in a large configuration space consisting of eleven major shells

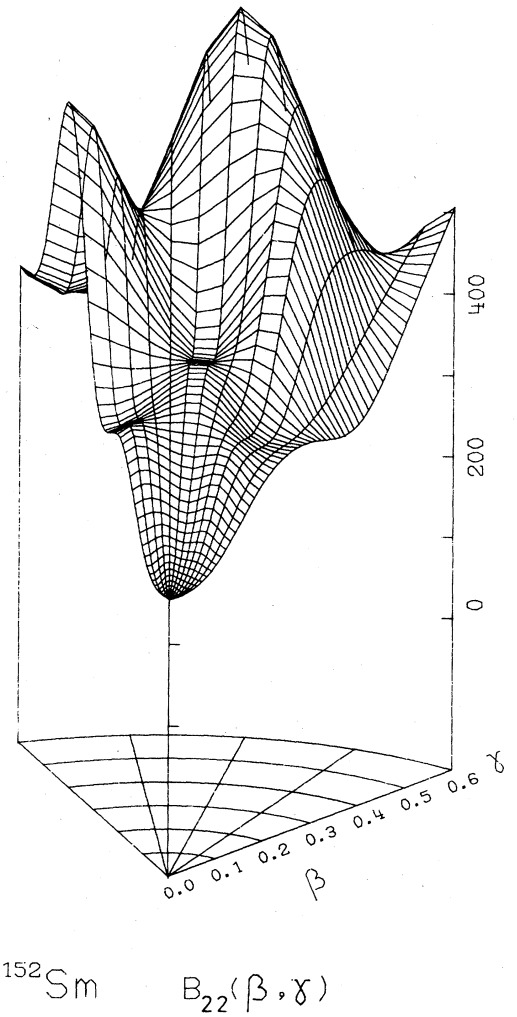

FIG. 7. Inertial function $B_{22}(\beta,\gamma)$ of ^{152}Sm. See Fig. 5 caption for further details.

for protons and eleven for neutrons. The m mixing due to the γ degree of freedom and the $\Delta N=2$ mixing due to the deformations are fully taken into account. The deforming part of the triaxial oscillator Hamiltonian is diagonalized for each nuclear shape, i.e., for each of the 92 points of the β-γ mesh used for the numerical solution[11,12] of the Bohr Hamiltonian. Then, the deformed-single-particle matrix elements of various single-particle operators (H_{sp}, Q_{20}, Q_{22}, **J**, **S**) are computed for each shape. This calculation of over 23 million wave functions and matrix elements represents the major computational effort of the DDM. If this had to be repeated for each nucleus, then the DDM calculation would be almost as time consuming as the HFB calculation. However, a scaling method has been found[13] which requires the computation of the single-particle matrix elements only once for all nuclei.

All nucleons are treated equally. The usual division into an inert core and an active cloud is avoided (also in the HFB method discussed previously, as well as in the Nilsson[17] method). No effective charges, or effective gyromagnetic ratios, or core renormalization parameters are needed. All model parameters (spherical single-particle energies, spherical oscillator frequencies, and pairing force strengths) are of a global nature, i.e., they have previously prescribed strengths and Z-A dependences.

This model has been employed for a global study[13] of selected even-even nuclei spanning light-medium-heavy, spherical-transitional-deformed nuclei with $A=12$—240. The same model has been employed for the predictions[8] of fission lifetimes of transuranic and superheavy nuclei ($A=240$—350).

IV. FORM FACTOR CALCULATIONS

In this section we present in the framework of the CCM, the calculations of the various coupling potentials between different channels. Our formulation of these calculations is made in a general way and can be applied to a great variety of scattering cross-section calculations. However, the formalism presented here does not include complicated contributions from spin-flip and exchange processes.

A. Central nuclear form factors

We assume that the baryon-nucleus interaction can be represented by a phenomenological potential. This potential includes deformed complex terms of a Woods-Saxon form and its derivative. In the following, we denote by i a set of usual deformation and asymmetry parameters: β_i and γ_i. For a given value of i, the deformed Woods-Saxon potential is written as

$$V_i(r,\theta',\varphi')=V_0/(1+\exp\{[r-R_i(\theta',\varphi')]/a\}) , \tag{17}$$

where $R_i(\theta',\varphi')$, the nuclear radius in the intrinsic-coordinate system, is given by

$$R_i(\theta',\varphi')=r_0A^{1/3}\{1+\beta_i\cos\gamma_i Y_{20}(\theta')+\beta_i\sin\gamma_i[Y_{22}(\theta',\varphi')+Y_{2,-2}(\theta',\varphi')]/2^{1/2}\} . \tag{18}$$

We then expand $V_i(r,\theta',\varphi')$ in terms of spherical harmonics,

$$V_i(r,\theta',\varphi')=V_0\sum_{\lambda\ \text{even}}\sum_{m=0}^{\lambda}[2(1+\delta_{m0})]^{-1/2}V_{i\lambda}^{m}(r)[Y_{\lambda m}(\theta',\varphi')+Y_{\lambda,-m}(\theta',\varphi')] . \tag{19}$$

Transforming Eq. (19) into the space-fixed system and after some algebra we obtain

$$V_i(r,\theta,\varphi)=V_0\sum_{\lambda\ \text{even}}[2(1+\delta_{\lambda 0})]^{-1/2}\times\sum_{m=0}^{\lambda}V_{i\lambda}^{m}(r)(Q_{\lambda m}\cdot Y_\lambda)\ . \tag{20}$$

In the last expression we have followed the definition of Tamura.[2] The transition operator $Q_{\lambda m}$ is an operator which operates only on the coordinates of the target nuclei and is given by

$$Q_{\lambda m}=D^{\lambda}_{,m}+D^{\lambda}_{,-m}\ , \tag{21}$$

whereas Y_λ is a transition operator which operates only on the coordinates of the projectile.

Using Eqs. (6) and (7) for the target nucleus wave functions and Eq. (20) for the target-projectile interaction, the calculation of the nuclear form factor is straightforward. For a given value of J and π (the angular momentum and parity of the whole system), we denote by $(nljI)$ the quantum numbers of a channel corresponding to the nth state of the target nucleus, and by s the spin of the projectile. The coupling matrix element between two channels is then given by

$$V_{nljI,n'l'j'I'}(r)=V_0\sum_{\lambda\ \text{even}}^{I+I'}A(ljI,l'j'I';\lambda Js)W^{\lambda}_{nI,n'I'}(r)\ , \tag{22}$$

where the factor $A(ljI,l'j'I';\lambda Js)$ is completely geometrical [see Eq. (28) of Ref. 2]. The form factor $W^{\lambda}_{nI,n'I'}(r)$ contains all the dynamical and structural information of the problem and is given by

$$W^{\lambda}_{nI,n'I'}(r)=\sum_{K,K',i}A_{nIK}(i)A_{n'I'K'}(i)\times\sum_{m=0}^{\lambda}V_{i\lambda}^{m}(r)\langle\Phi^{I}_{MK}||Q_{\lambda m}||\Phi^{I'}_{M'K'}\rangle\ . \tag{23}$$

The reduced matrix element appearing in Eq. (23) can be easily calculated using the properties of Wigner rotation matrices (see, for example, Appendix A of Ref. 33).

B. Comparisons with the form factor calculations in other collective models

In most of the conventional applications of the collective model, the deformation and asymmetry variables have only one fixed value each. We can also restrict the summation on the shape parameter index i in Eq. (23) to only one value and choose the corresponding (β,γ) values so as to obtain the conventional form factors: $\beta\neq 0$, $\gamma=0$ for a prolate rotator; $\beta\neq 0$, $\gamma=60°$ for an oblate rotator; $\beta\neq 0$, $0°<\gamma<30°$ for a triaxial rotator; $\beta\neq 0$, $\gamma=30°$ for a quadrupole harmonic vibration. In our actual calculations the summation over all relevant values of the shape variables allows, for the various channels, the possibility of shape coexistence.

In recent years, Arima and Iachello[34] have developed the interacting boson approximation (IBA) model. This model is an attempt to provide a microscopic description of low-lying collective states in medium- and heavy-mass nuclei. The possibility to describe nuclear form factors, or nucleon density distributions using this model was investigated most extensively at a phenomenological level. We mention, however, that schematic calculations have been performed[35] with single-particle wave function in a harmonic oscillator potential. In the case of nucleon scattering cross section calculations, this possibility was investigated at various times (see Deason *et al.*[36]). In their coupled channel calculations of 35 MeV proton scattering cross sections from ^{194,196,198}Pt, these authors[36] assumed a phenomenological radial dependence of the form factors and took the relative transition strengths (or reduced matrix elements) from the IBA model. For form factors and nucleon density distribution calculations, the IBA model suffers from the fact that the boson density distribution cannot be easily calculated and is generally deduced from electron scattering data. One of the most interesting features of our calculations is that the radial dependence of the form factors is closely related [see Eq. (23)] to the nuclear structure wave functions. Thus, the form factors can differ, even for the same multipole, from state to state. This behavior can be illustrated by the results presented in Figs. 8(a) and (b). There we have shown for ^{24}Mg, the computed values of the form factor $W^{\lambda}_{nI,n'I'}(r)$. Moreover, in going from one nucleus to another, the form factors can differ in shape. We have exhibited in Fig. 8(c) the radial dependence of the quadrupole reorientation matrix element calculated for the first 2^+ state of ^{148,154}Sm. Finally, the curves reported in Fig. 8(d) correspond to the radial dependence of the monopole transition form factor between the $0^+_{\text{g.s.}}$ (ground state) and the 0^+_β (beta bandhead) of ^{24}Mg and ^{28}Si. The radial dependences of these monopole transition form factors are similar to those of the second derivative of a Woods-Saxon potential. Moreover, the radial dependences of the diagonal monopole form factors computed for the two 0^+ states are similar to the diagonal part of the Woods-Saxon potential. In the case of the monopole 0^+-0^+ transitions, Eqs. (22) and (23) reduce to

$$V_{nlj0,n'lj0}(r)=V_0W^{0}_{n0,n'0}(r)\ , \tag{24}$$

$$W^{0}_{n0,n'0}(r)=\sum_i A_{n00}(i)A_{n'00}(i)V^{0}_{i0}(r)\ . \tag{25}$$

The various radial dependences of the monopole transition form factors of Eq. (25), come from the weighting of the shape dependent $V^0_{i0}(r)$ by the nuclear structure amplitude factors $A_{n00}(i)$ and $A_{n'00}(i)$.

C. Coulomb and spin-orbit potentials

In our coupled channel calculations of 120 MeV ^{4}He-scattering cross sections from ^{24}Mg and ^{28}Si, the Coulomb excitation of the collective bands was neglected since it had little effect[37] on the shapes of the angular distributions although it did affect their magnitudes slightly. Thus, the Coulomb potential adopted was that of a homogeneous charged sphere. In the case where Coulomb excitation processes must be taken into account, the deformed Coulomb potential can be treated in the body-centered

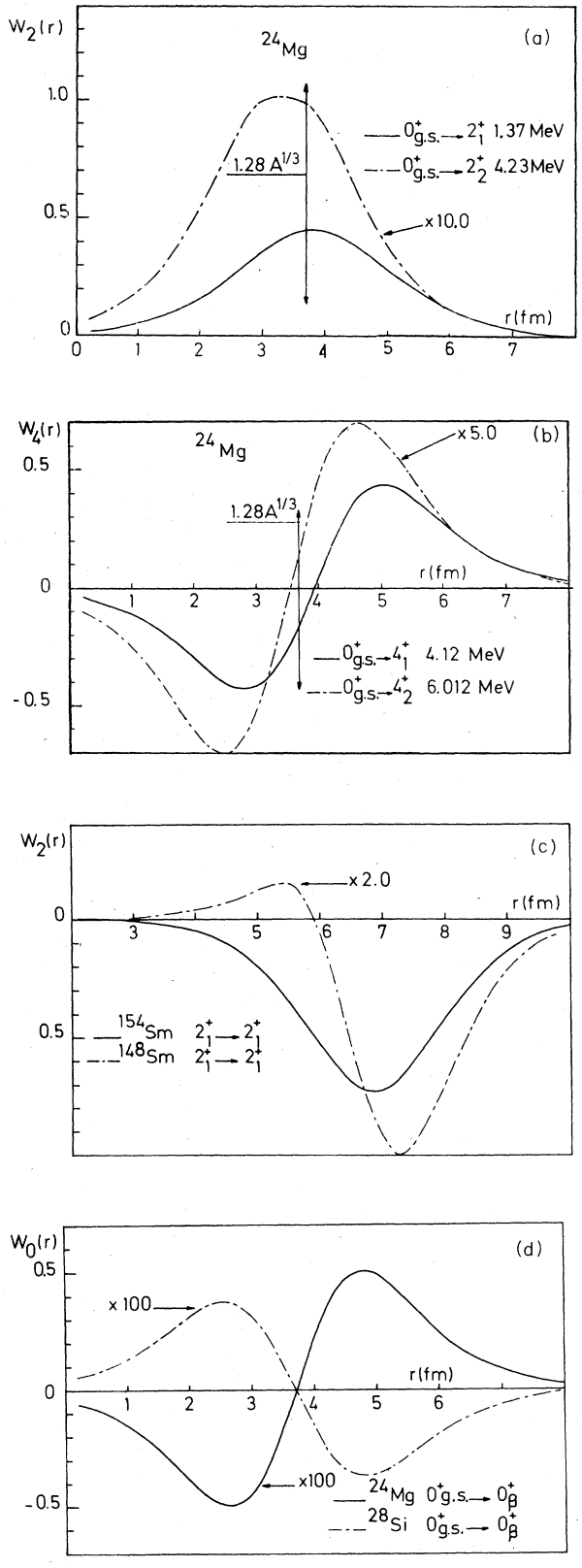

FIG. 8. Radial dependence of form factors $W^{\lambda}(r)$. (a) ^{24}Mg: $\lambda=2$. (b) ^{24}Mg: $\lambda=4$. (c) ^{148,154}Sm: $\lambda=2$. (d) ^{24}Mg, ^{28}Si: $\lambda=0$.

system in the same manner as the nuclear potential $V(r,\theta',\varphi')$.

In our coupled channel calculations of neutron scattering cross sections from Sm isotopes, we have included a phenomenological spin-orbit potential

$$V_{\rm SO}(r)=V_{\rm SO}[\hbar/(m_{\pi}c)]^2(1/r)[dV(r)/dr]\mathbf{l}\cdot\boldsymbol{\sigma} \tag{26}$$

where $V(r)$ is a spherical Woods-Saxon potential. The deformed spin-orbit interaction was neglected for the following reasons: (i) Our coupled channel program cannot handle the possibility of a deformed spin-orbit interaction given as a full Thomas term[1,38]

$$-i[\hbar/(2m_{\pi}c)]^2\boldsymbol{\sigma}\cdot[\nabla V(r)\times\nabla] . \tag{27}$$

(ii) The potential $V(r)$ of Eq. (27) is a deformed potential with fixed deformation values (β,γ), whereas in our actual calculations, values of the deformation of the nuclear potential are not fixed. We are now investigating the possibility of generalizing the deformed spin-orbit interaction for variable shapes.

D. Numerical methods employed for form factor calculations

The crucial point in the numerical procedure used for the form factor calculations is the computation of $V^{m}_{i\lambda}(r)$ of Eq. (19). This computation must be made for each value of r, the 92 values of (β,γ), and for different channels (in the simplest case, the coupling of the $0^+,2^+,4^+$ states requires at least 14 real and imaginary transition potentials). Thus, the direct method of a two-dimensional integration over the angles (θ,φ) would consume large amounts of computer time. Raynal[39] has developed a very efficient method for such computations. This method, called "linear approximation," consists of first computing the inverse of M, a real square matrix of order N with elements M_{jk} [where the index k denotes a set of values (λ,m)] of the form

$$M_{jk}=\{1/[2(1+\delta_{\lambda 0})]\}^{1/2}[Y_{\lambda m}(\theta_j,\varphi_j)+Y_{\lambda,-m}(\theta_j,\varphi_j)] , \tag{28}$$

and then computing the $V^{m}_{i\lambda}(r)$ as

$$V^{m}_{i\lambda}(r)=\sum_{j=1}^{N}(M_{jk})^{-1}V_i(r,\theta_j,\varphi_j) , \tag{29}$$

where we recognize the matrix elements of the inverted matrix.

We have implemented this method in our computer code. The accuracy of this linear expansion approximation was investigated using two different tests: (i) The dimension of the square matrix M was varied ($N=36,45$) to evaluate truncation effects of the linear expansion. (ii) Direct comparisons with the two-dimensional integration procedure were made. This approximation was found to give accurate results for all the channel potentials needed for our coupled channel calculations (up to $\lambda_{\max}=m_{\max}=8$).

The numerical calculations of the form factors were tested using only one set of values of the deformation

variables (β,γ) via comparisons with various results obtained using the code ECIS of Raynal.[39]

V. COUPLED CHANNELS CALCULATIONS

These form factor calculations were incorporated into our coupled channels computer code. This code is essentially the same as was previously used for semimicroscopic calculations of nucleon elastic and inelastic scattering cross sections for spherical[40] or for heavy well-deformed nuclei.[24] Because of computer storage requirements, the number of levels which could be coupled in was limited to six and the number of different radial form factors [see Eq. (23)] for each individual nuclear potential was restricted to 60. The nuclear potentials were expanded in multipoles [see Eq. (19)] up to $\lambda_{\max}=8$, and complex coupling terms were employed throughout this work.

The optical model parameters of the Woods-Saxon potential, and of its first derivative, were obtained from previously published CCM or DWBA analysis of inelastic baryon scattering. These parameters are listed in Table I. Because of the inclusion of inelastic channels in our CCM analysis, the imaginary part of the ^{4}He-^{28}Si potential had to be reduced from 24.6 to 20.7 MeV. This reduction is similar to the one obtained by Van der Borg *et al.*[37] in their CCM analysis of inelastic ^{4}He scattering from ^{24}Mg.

A. Analysis of 120 MeV ^{4}He-scattering data for ^{24}Mg

The experimental data were obtained by Van der Borg *et al.*[37,41] There, in the framework of the triaxial rotor model, a conventional coupled channel analysis was also presented. For the calculations of the nuclear form factors, these authors have employed a first-order Taylor expansion of $V(r,\theta',\varphi')$ in terms of $\beta\sin\gamma[Y_{22}(\theta',\varphi')+Y_{2-2}(\theta',\varphi')]$. As our expansion procedure is different [see Eq. (19)], a direct comparison of our calculations with theirs cannot be presented.

We have performed two sets of coupled channel calculations, assuming two different coupling schemes. In the first set of calculations, the $0^+,2^+,4^+$ states of the ground state band and the $2^+_\gamma,3^+_\gamma,4^+_\gamma$ states of the excited γ band were coupled. In the second set of calculations, the $0^+_\beta,2^+_\beta$ of the excited β band were coupled instead of the 3^+_γ and 4^+_γ states. Note that in the first case we had to calculate 53 real and imaginary form factors, while this number was reduced to 43 in the second case. Because of the considerable computer time required for the form factor and the coupled channel calculations, we have not undertaken any optical model potential (OMP) parameter search.

The results corresponding to the first set of calculations are presented together with the experimental data in Fig. 9. The full curves correspond to calculated cross sections obtained without any adjustments of the OMP parameters or of the nuclear form factors. While the agreement obtained for the $0^+,2^+$ states of the ground state bands and for the 2^+_γ state of the γ band are rather good, the calculated angular distributions for the $3^+_\gamma,4^+_\gamma$ states of the γ band are quite off. For the 4^+ state of the ground band, the agreement is not very good either. We have tested that coupling the 6^+ state of the ground state band and excluding the 3^+_γ and 4^+_γ states does not affect the results significantly. As mentioned in Ref. 37, the form factor for the 4^+ state of the ground state band is very sensitive to variations of the imaginary potential depth. We have observed that an increase of that depth does decrease the magnitude of the calculated 4^+ cross section, but it also alters the fit obtained for the elastic scattering cross section. We think that the discrepancy between the calculated results and the experimental data could come in part from the current choice of the OMP parameters and in part from the nuclear structure wave function calculations.

In earlier studies (see, for example, Ref. 37), it was already found that the 4^+_γ state was too weakly excited and required a very strong coupling to the ground state. In order to test this possibility, we multiplied the $0^+_{\text{g.s.}}\rightarrow 4^+_\gamma$ transition form factor by a renormalization factor, and

TABLE I. Optical model parameters. The parameters (except for minor adjustments in the strengths of the imaginary potentials) have been taken from Ref. 37 for ^{24}Mg, Ref. 41 for ^{28}Si, and Ref. 42 for Sm nuclei.

	^{24}Mg $E_\alpha=120$ MeV	^{28}Si $E_\alpha=120$ MeV	Sm $E_n=0.75-15$ MeV	
V_R (MeV)	100	109.7	$46.3-0.22E$	
a_R (fm)	0.78	0.81	0.65	
r_R (fm)	1.28	1.25	1.25	
W_V (MeV)	19	20.7	0.0	($E<8$ MeV)
			$-1.28+0.16E$	($E>8$ MeV)
a_V (fm)	0.71	0.51	0.65	
r_V (fm)	1.60	1.63	1.25	
W_D (MeV)			$2.3+1.1E^{1/2}$	($E<8$ MeV)
			$5.32+0.056E^{1/4}$	($E>8$ MeV)
a_D (fm)			0.58	
r_D (fm)			1.25	
V_{so} (MeV)			7.5	
a_{so} (fm)			0.65	
r_{so} (fm)			1.25	
r_c (fm)	1.3	1.3		

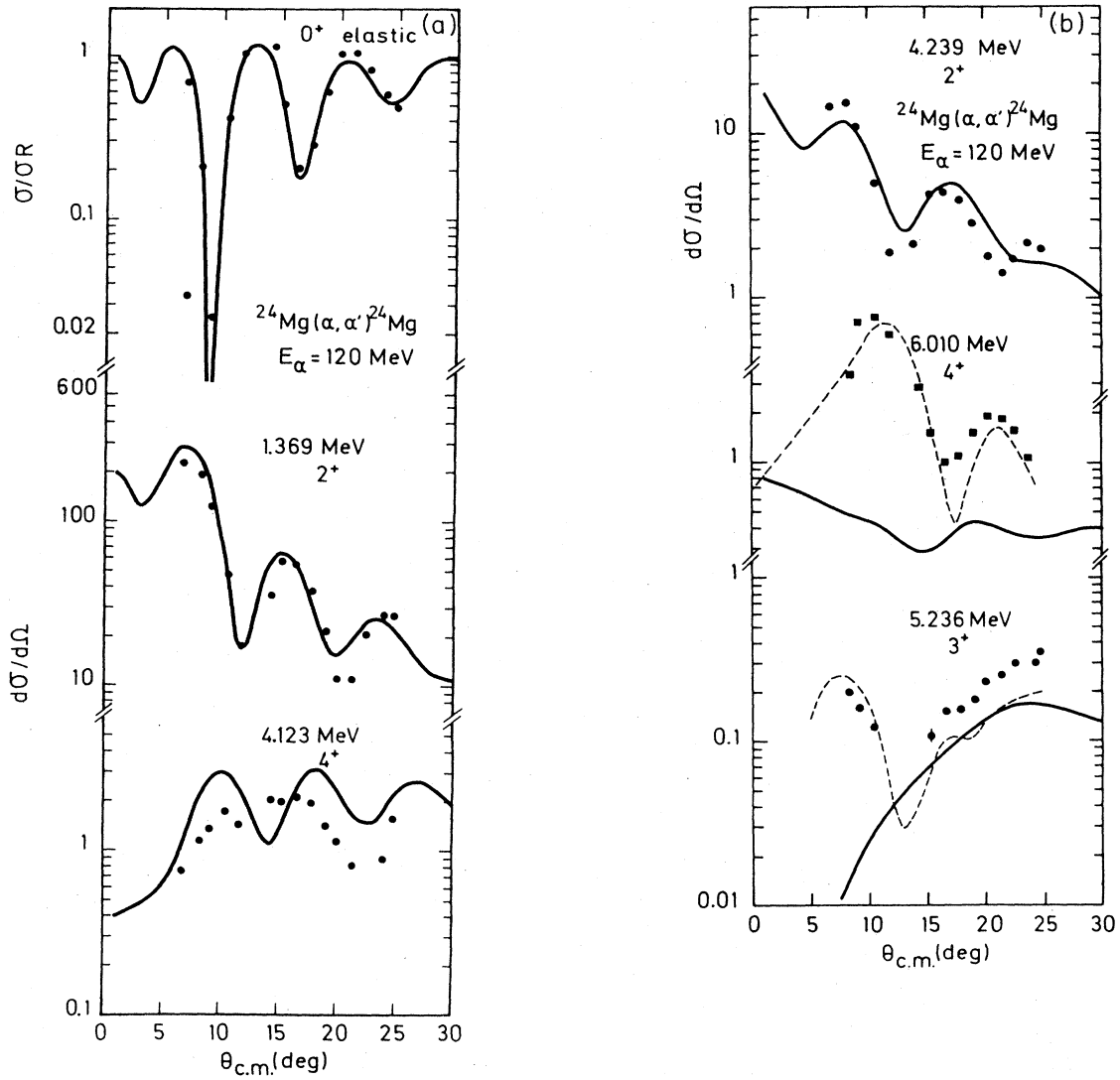

FIG. 9. Angular distributions for ^{4}He scattering from (a) the ground-state band, and (b) from the γ-band states of ^{24}Mg. The solid curves are results of the present coupled channel calculations. See the text for discussion of the dashed curves. The experimental data are from Ref. 41.

varied this factor until a satisfactory agreement was reached. The results obtained, using a value of 5 for that factor, are shown, as dashed curves in Fig. 9. We observe that for the 3^+_γ, the calculated curve changes in shape as well as in magnitude. However, that calculated curve does not reproduce the second experimental oscillatory pattern. The radial dependence of the renormalized form facor was shown in Fig. 8(b). We note that it differs from the one adopted, for the same transition, by Van der Borg *et al.*[37] (first derivative of a Woods-Saxon form). We think that the discrepancies observed for the 4^+_γ and 3^+_γ states come from the nuclear structure calculations. In those calculations, these states are respectively located at 9.98 and 8.22 MeV excitation energies, whereas the corresponding experimental values are 6.01 and 5.24 MeV.

The results obtained for the second set of calculations are presented in Fig. 10. While the agreement obtained for the 0^+_β state of the β band is quite good, the calculations for the 2^+_β state are off by more than an order of magnitude. In the nuclear structure calculations, the 0^+_β and 2^+_β states are respectively located at 5.95 and 8.91 MeV excitation energies, whereas the corresponding experimental values are 6.43 and 7.45 MeV. The fact that the predicted excitations for 0^+_β and 2^+_β are respectively stronger and much weaker than the experimental data, can be correlated with the differences between the experimental and the calculated excitation energies for these states. The baryon excitation of the ^{24}Mg β band was the subject of a recent analysis presented by Harakeh and De Leo.[43] These authors concluded that the 0^+_β excitation can be satisfactorily explained only if a monopole breathing mode form factor is included in addition to the monopole β-vibration form factor. As our calculation reproduces, for that state, satisfactorily the experimental diffraction pattern, we think that the inclusion of a breathing mode form factor is not necessary. Finally, we recall that the

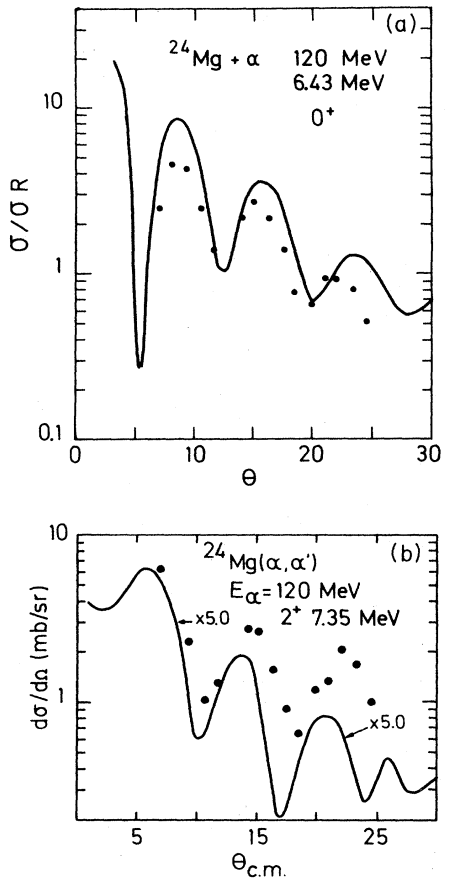

FIG. 10. Angular distributions for ^{4}He scattering from (a) the 0^+_β and (b) the 2^+_β states of ^{24}Mg. The solid curves are results of the present coupled channel calculations. The experimental data are from Ref. 41.

radial dependence of the present form factor is presented in Fig. 9.

B. Analysis of the 120 MeV scattering data for ^{28}Si

The experimental data were obtained by Van der Borg *et al.*[41] in a similar way as for ^{24}Mg. These authors have presented a coupled channel calculation in the framework of the vibrational model for the ground state and the first excited 2^+, 4^+, and 0^+ states, whereas DWBA calculations were undertaken for the remaining excited states. We mention that an equally good fit to the ground state band (0^+,2^+,4^+) states can be obtained in the vibrational[45] or the rotational[44] scheme.

The present nuclear structure wave function calculations indicate that substantial band mixing (especially between the $K=0,2,4$ components) occurs for all the excited levels. On the basis of the largest K components, we have made the following classification:

g.s. band: 0^+,2^+(1.78 MeV), 4^+(4.62 MeV) ;

γ band: 3^+(6.28 MeV), 2^+(8.26 MeV) ;

β band: 0^+(4.98 MeV), 2^+(7.38 MeV) .

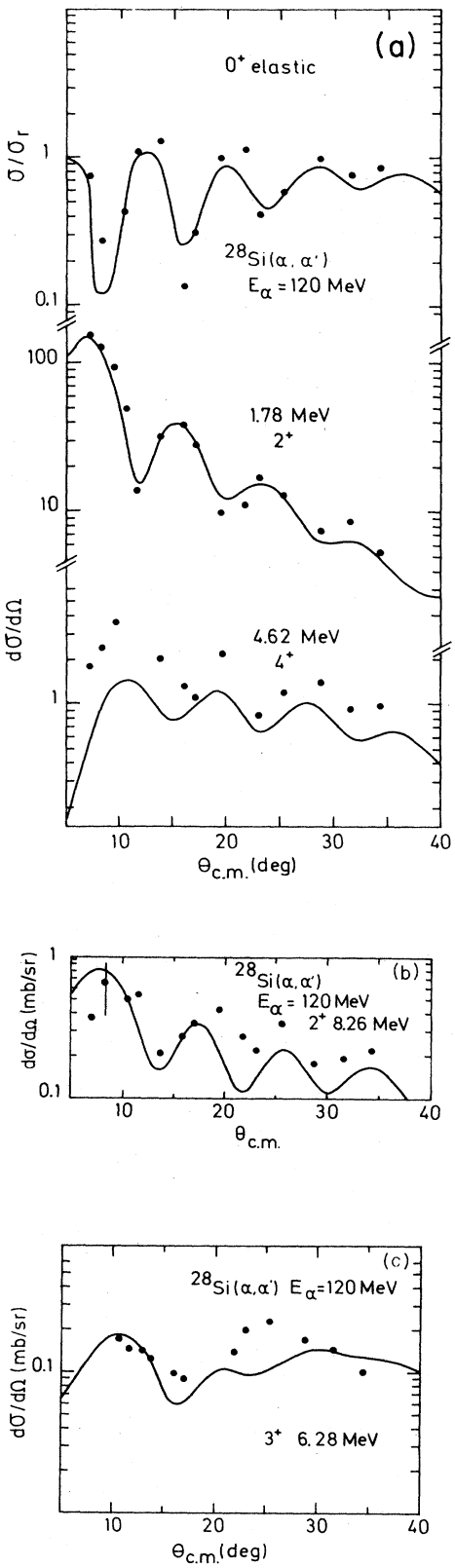

FIG. 11. Angular distributions for ^{4}He scattering from (a) the ground-state band, (b) the 2^+_γ state, and (c) the 3^+_γ state of ^{28}Si. The solid curves are results of the present coupled channel calculations. The experimental data are from Ref. 41.

The reason for our choice of the 2^+ state of the γ band will be explained in the following.

In the first set of calculations, we have included the members of the g.s. and the γ band. The calculated angular distributions for these states, together with the experimental data, are shown in Fig. 11. The agreement is good for the 0^+ and the 2^+ states of the g.s. band. Note that the 4^+ predicted cross sections miss the data in magnitude, but are generally in phase with them. The possibility of describing the 2^+ state at 8.26 MeV as the 2^+_γ state of the γ band comes from the magnitude and the shape between 30° and 40° of the calculated cross sections. This appears clearly when looking at the experimental angular distributions for various 2^+ states of ^{28}Si, as reported in Fig. 13 of Ref. 41. The prediction for the 3^+_γ angular distribution is only fair; the calculation misses the experimental pattern of the second maximum. Since the 3^+_γ state is only excited by two-step processes in the present calculation, the coupling $4^+_{g.s.} \rightarrow 3^+_\gamma$ is very important. As the $4^+_{g.s.}$ wave function has $K=0$, 2, and 4 components, the strength of this direct coupling is greatly enhanced. However, this is not the case for the $4^+_{g.s.}$ of ^{24}Mg which has only a pure $K=0$ component.

In a second set of calculations, we have included the members of the g.s. and the β bands. As can be seen in Fig. 12, the prediction of the 0^+_β angular distribution is only fair; the calculation does not reproduce the pattern and slope of the experimental data beyond about 17°. In

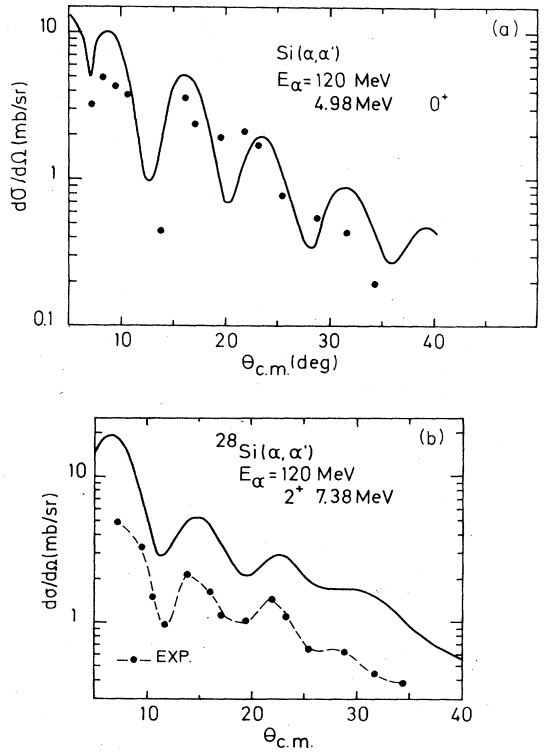

FIG. 12. Angular distributions for ^{4}He scattering from (a) the 0^+_β and (b) the 2^+_β states of ^{28}Si. The solid curves are the results of the present coupled channel calculations. The dashed curve has been drawn to guide the eye through the experimental data taken from Ref. 41.

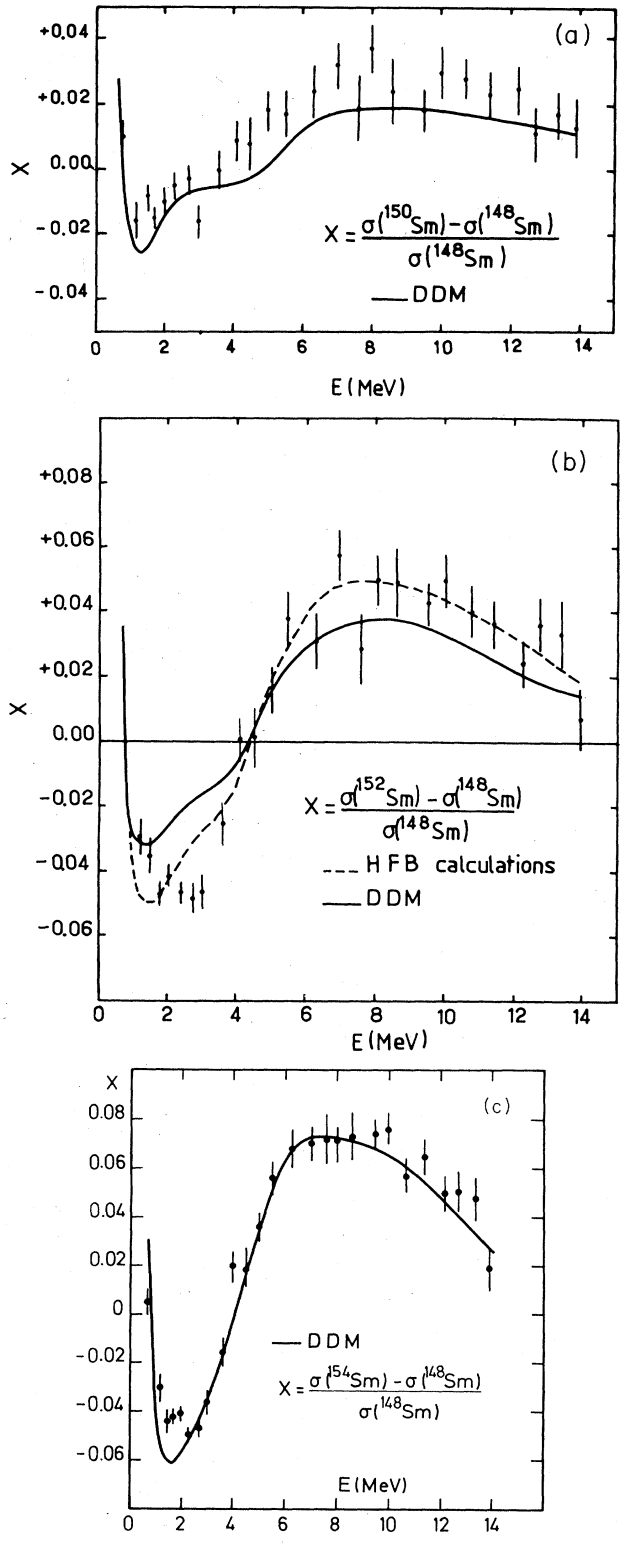

FIG. 13. Fractional differences of total neutron cross sections of (a) ^{150}Sm, (b) ^{152}Sm, and (c) ^{154}Sm relative to ^{148}Sm. The solid (dashed) curves are results of the ECCM combined with the DDM (HFB). Both types of calculations included the coupling of the ground state (0^+) and the first excited state (2^+). The experimental data are from Ref. 46.

the same figure, we have presented for the 2^+ state the calculated and the experimental angular distributions. In order to facilitate shape comparisons between them, we have drawn a dashed line though the experimental data. We can see that the predicted angular distribution reproduces the experimental pattern fairly well. On the other hand, the predicted excitation strength is too high by a factor of 3. This could come from the fact that in the actual nuclear structure calculation, this state is located at 6.43 MeV excitation energy, whereas the corresponding experimental energy is 7.38 MeV.

C. Analysis of 0.75–15 MeV neutron total cross sections for Sm isotopes

The nuclear deformation may be deduced from an analysis of baryon elastic and inelastic scattering cross sections, from the analysis of total neutron cross sections, and also from total neutron cross section differences for pairs of isotopes. The effect of nuclear deformation on neutron total cross sections was first measured at 0.35 MeV for an oriented target, ^{165}Ho.[45] Later, total neutron cross section differences for unoriented targets were measured in the energy range 0.75–15 MeV for even Sm isotopes.[46] The interpretations of these last experimental findings were made[46] via coupled channel calculations in the frame of the rotational or the vibrational model. We present here, so as to test our model, a brief analysis using deformation dependent wave functions. The nuclear wave functions employed for that purpose were calculated in the DDM for ^{148,150,152,154}Sm and from the HFB method for ^{152}Sm The OMP parameters displayed in Table I are for ^{154}Sm. For the other isotopes, the OMP parameters can be obtained using the usual isospin dependence for the potential strengths: $V_1=18$ MeV and $W_{D1}=9$ MeV. The calculated neutron total cross sections for ^{148}Sm are in fair agreement with experiment. The calculated neutron total cross section differences between ^{150}Sm, ^{152}Sm, ^{154}Sm, and ^{148}Sm are presented in Fig. 13 together with the experimental values of Ref. 46. There it was surmised that the change in the relative difference between the 7 MeV maximum and the 2 MeV minimum is a measure of the difference in deformation between these isotopes. As the calculated curves reproduce, in a satisfactory way, the relative differences, we can conclude that the collective properties of these isotopes are consistent with our model.

Finally, the angular distributions, computed using the present optical model parameters and wave functions, are in good agreement (see, for example, Figs. 10 and 11 of Ref. 13) with recent neutron elastic and inelastic scattering data[42] for these Sm isotopes.

VI. CONCLUSIONS

We have presented an extended coupled channel method for baryon scattering cross-section calculations of great versatility. This method can be employed for nuclei which can be anywhere in between the two limits of the Bohr-Mottelson model. Moreover, it can also be employed for a nucleus with the coexistence of different shapes at different excitations.

For practical reasons, the optical potential was not treated in a microscopic way, and thus some phenomenological parameters are still needed. These parameters can be easily determined from a fit to the elastic scattering data only. However, the present model differs from the phenomenological collective models in the radial dependence of the various form factors. These form factors are closely related to the nuclear structure wave functions and can differ, even for the same multipole, from state to state.

As illustrative examples of the extension of the coupled channel method, we have presented form factors, angular distributions, and cross sections for baryon scattering from several nuclei: ^{24}Mg, ^{28}Si, and ^{150,152,154}Sm. We have shown that the same model can be used, without any additional parameters, for scattering from the ground-state band, the gamma band, as well as the beta band. Although some problems remain because of less accuracy in the nuclear structure wave functions of higher states, it is generally not necessary to use any renormalization factors.

It would be interesting to test more accurately the radial dependence of the form factors by comparisons of calculated results with the experimental data for more energetic projectiles (for instance, 500 MeV protons). However, our main conclusion is that the few illustrative examples already indicate that the method presented here provides a powerful tool for analyzing baryon scattering from various even-even nuclei.

ACKNOWLEDGMENTS

One of us (K.K.) thanks M. G. Mustafa for hospitality at Lawrence Livermore Laboratory during the summers of 1981 and 1982. This research was supported by the Tennessee Technological University Endowment Fund via University Professor of Physics Research Grant.

[1]G. R. Satchler, *Direct Nuclear Reactions* (Oxford University, New York, 1983).
[2]T. Tamura, Rev. Mod. Phys. **37**, 679 (1963).
[3]A. Bohr and B. R. Mottelson, *Nuclear Structure* (Benjamin, New York, 1975).
[4]H. Rebel, G. W. Schweimer, D. Habs, and H. J. Gils, Nucl. Phys. **A225**, 457 (1974).
[5]G. Gneuss and W. Greiner, Nucl. Phys. **A71**, 449 (1971); G. Gneuss, U. Mosel, and W. Greiner, Phys. Lett. **30B**, 397 (1969); **31B**, 269 (1970).
[6]A. Bohr, K. Dan. Vidensk. Selsk. Mat.-Fys. Medd. **26**, No. 14 (1952).
[7]K. Kumar, Prog. Part. Nucl. Phys. **9**, 233 (1983); *Nuclear Models and the Search for Unity in Nuclear Physics* (Columbia University, New York, 1984).
[8]K. Kumar and M. G. Mustafa, in *Proceedings of the International Conference on Nuclear Physics, Florence, Italy, 1983* (Tipografia Compositori, Bologna, 1983), Vol. I, p. 626; Bull. Am. Phys. Soc. **29**, 757 (1984).
[9]J. Dechargé and D. Gogny, Phys. Rev. C **21**, 1568 (1980).

[10]M. Girod, K. Kumar, B. Grammaticos, and P. Aguer, Phys. Rev. Lett. **41**, 1765 (1978).
[11]K. Kumar and M. Baranger, Nucl. Phys. **A92**, 608 (1967).
[12]K. Kumar, in *The Electromagnetic Interaction in Nuclear Spectroscopy,* edited by W. D. Hamilton (North-Holland, Amsterdam, 1975), p. 55.
[13]K. Kumar, in *Structure of Medium-Heavy Nuclei 1979,* Conf. Ser. No. 49 (The Institute of Physics, Bristol, 1979), p. 169.
[14]Ch. Lagrange, M. Girod, B. Grammaticos, and K. Kumar, Lawrence Berkeley Laboratory, University of California, Berkeley, Report LBL-11118, 1980, Vol. I, p. 352.
[15]Ch. Lagrange, M. Girod, B. Grammaticos, and K. Kumar, in *Proceedings of the International Conference on Nuclear Physics, Florence, Italy, 1983* (Tipografia Compositori, Bologna, Italy, 1983), Vol. I, p. 463.
[16]A. S. Davydov and G. F. Filippov., Nucl. Phys. **8**, 237 (1958).
[17]S. G. Nilsson, K. Dan. Vidensk. Selsk. Mat.-Fys. Medd. **29**, No. 16 (1955).
[18]G. Ripka, Adv. Nucl. Phys. **1**, 183 (1968).
[19]B. Giraud and B. Grammaticos, Nucl. Phys. **A233**, 373 (1974).
[20]D. R. Inglis, Phys. Rev. **97**, 701 (1955).
[21]A. K. Kerman, Ann. Phys. (N.Y.) **12**, 300 (1961).
[22]L. S. Kisslinger and R. A. Sorensen, K. Dan. Vidensk. Selsk. Mat.-Fys. Medd. **32**, No. 9 (1960).
[23]F. A. Brieva and B. Z. Georgiev, Nucl. Phys. **A308**, 27 (1978).
[24]Ch. Lagrange and M. Girod, J. Phys. G **9**, L97 (1983).
[25]R. S. Mackintosh, Nucl. Phys. **A307**, 365 (1978).
[26]B. Z. Georgiev and R. S. Mackintosh, Nucl. Phys. **A307**, 377 (1978).
[27]J. S. Vaagen and K. Kumar, J. Phys. G **5**, 1211 (1979).
[28]C. F. Maguire, D. L. Hendrie, U. Jahnke, J. Mahoney, D. K. Scott, J. S. Vaagen, R. J. Ascuitto, and K. Kumar, Phys. Rev. Lett. **40**, 358 (1978).
[29]M. Girod and B. Grammaticos, Phys. Rev. C **27**, 2317 (1983).
[30]M. Girod and B. Grammaticos, Nucl. Phys. **A330**, 40 (1979).
[31]V. M. Strutinsky, Yad. Fiz. **3**, 614 (1966) [Sov. J. Nucl. Phys. **3**, 449 (1966)].
[32]W. D. Myers and W. J. Swiatecki, Ann. Phys. (N.Y.) **84**, 186 (1974).
[33]H. Rebel, G. Hauser, G. W. Schweimer, G. Nouiki, W. Wiesner, and D. Hartmann, Nucl. Phys. **A218**, 13 (1974).
[34]F. Iachello and A. Arima, Phys. Lett. **53B**, 309 (1974); F. Iachello, Nukleonika **22**, 107 (1977); A. Arima and F. Iachello, Ann. Phys. (N.Y.) **99**, 99 (1976).
[35]T. Otsuka, A. Arima, and F. Iachello, Nucl. Phys. **A309**, 1 (1978).
[36]P. T. Deason, C. H. King, R. M. Ronningen, T. L. Khoo, F. M. Bernthal, and J. A. Nolen, Jr., Phys. Rev. C **23**, 1414 (1981).
[37]K. Van der Borg, M. N. Harakeh, and B. S. Nillson, Nucl. Phys. **A325**, 31 (1979).
[38]H. Sherif and J. S. Blair, Phys. Lett. **28B**, 961 (1968).
[39]J. Raynal, private communication; J. Raynal, computer code ECIS 79 (unpublished).
[40]Ch. Lagrange and J. C. Brient, J. Phys. (Paris) **44**, 27 (1983).
[41]K. Van der Borg, M. N. Harakeh, and A. Van der Woude, Nucl. Phys. **A365**, 243 (1981).
[42]M. T. McEllistrem, R. E. Shamu, J. Lackhar, G. Haouat, Ch. Lagrange, Y. Patin, J. Sigaud, and F. Cocu, Phys. Rev. **151**, 927 (1977).
[43]M. N. Harakeh and R. De Leo, Phys. Lett. **117B**, 377 (1982).
[44]H. Rebel, G. W. Schweimer, J. Specht, G. Schatz, R. Löhken, D. Habs, G. Hauser, and H. Klewe-Nebenius, Phys. Rev. Lett. **26**, 119 (1971).
[45]R. Wagner, P. D. Miller, T. Tamura, and H. Marshak, Phys. Rev. **139**, B29 (1965).
[46]R. E. Shamu, E. M. Bernstein, J. J. Ramirez, and Ch. Lagrange, Phys. Rev. C **22**, 18 (1980).